Noise Mitigation in Supersonic Jets Using Plasma Actuators

M. Samimy, J.-H. Kim, M. Kearney-Fischer, and I. Adamovich
Gas Dynamics and Turbulence Laboratory
Department of Mechanical Engineering, The Ohio State University
Columbus, Ohio 43235

Samimy.1@osu.edu

ABSTRACT

Noise mitigation has been in the forefront of research since the advent of jet engines. Supersonic commercial and especially supersonic military aircraft cannot take the advantages offered by large bypass ratio engines due to significant performance degradation. Therefore, other control techniques must be utilized to satisfy the more recent and looming future stringent noise regulations. A class of plasma actuators has recently been developed at the Ohio State University that offer significant promise. These actuators possess large bandwidth and can provide large amplitude perturbations enabling manipulation of various instabilities in high Reynolds number subsonic and supersonic jets for noise mitigation as well as mixing enhancement. A brief overview of the actuators and some results are presented in a perfectly-expanded Mach 1.3 axisymmetric jet.

1.0 INTRODUCTION

Understanding of jet noise sources and finding means to mitigate jet noise have offered considerable challenge to researchers and practitioners over the past several decades. On the commercial subsonic side, the U_j^8 dependency of the jet noise, where U_j is the jet velocity at the nozzle exit, based on Lighthill's scaling laws argument [Lighthill 1952], has been exploited to its full extent with significant success. However, additional reduction is necessary to meet the more stringent current and upcoming noise regulations. On the supersonic side, reducing velocity by using large bypass ratio engines is not a viable option, as it would adversely affect the aircraft performance. Therefore, other control options, both passive and active, have been pursued in recent years. The control technique is called passive, which is primarily based on nozzle geometrical modifications, if it is in place and on all the time, regardless of whether it is needed. In passive control, no energy is required to operate the device, and the technique cannot respond to changes in the flow/flight conditions. In addition, it incurs penalty even when it is not needed. Exhaust nozzles with mechanical chevrons and inverted velocity profiles are among passive technologies being explored [Martens and Haber 2008].

The control technique is termed active, if it could be turned on and off based on the need, and when it is on, it requires energy input. Fluidic chevrons [Martens and Haber 2008] and plasma actuators [Samimy et al. 2007a & b] are examples of active control devices. Active control can be divided into open-loop and closed-loop. In the latter, the actuator input is determined in real-time based on a model of the system and real-time measurements of the state of the flow [Samimy et al. 2007c]. In the former, which is more commonly used and is being used in the current research, the actuator input is predetermined, but could be changed in flight using, for example, a look-up table. The open-loop active control, active control hereafter, operates generally based on one of two principles. The first one involves generation of additional flow structures, primarily streamwise eddies, to alter the mixing and thus noise radiation. The use of fluidic chevrons falls into this category. The second one involves manipulation of jet instabilities and is detailed in Samimy et al. [2007a & b]. The use of plasma actuators, which is the subject of this paper, falls into this category.

Many researchers have used active control in low-speed and low Reynolds number jets via manipulation of jet instabilities for mixing or noise control [Kibens 1980, Zaman and Hussain 1980, Hussain and Zaman 1981]. Limited work has also been carried out in high-speed and high Reynolds number jets [Moore 1977, Jubelin 1980, Ahuja et al. 1982] and high-speed and low Reynolds number jets [Morrison and McLaughlin 1979]. Acoustic drivers were used in the first category and glow discharge type plasma actuators were used in the second category. Unfortunately, neither actuator has the required bandwidth or amplitude to control high-speed and high Reynolds number jets.

A class of actuators called Localized Arc Filament Plasma Actuators (LAFPAs) has been developed and used at the Ohio State University over the past several years to control high-speed and high Reynolds number jets [Samimy et al. 2004 and 2007a & b, Utkin 2007]. The primary mechanisms of plasma-based flow control, in general, include electrohydrodynamic (EHD) and magnetohydrodynamic (MHD) interactions, and thermal heating. EHD and MHD interactions involve flow entrainment by collisional momentum transfer from charged species accelerated by Coulomb and Lorentz forces, respectively. The primary mechanism of LAFPA is localized thermal heating that can provide necessary perturbations to control various instabilities in the jet. These actuators have sufficiently high bandwidth and authority, and can be distributed azimuthally to enable control of all three instabilities in an axisymmetric jet, namely initial free shear layer, jet column, and azimuthal.

The initial shear layer of a jet behaves similar to a planar free shear layer. Here the shear layer is referred to the mixing region between the jet exhaust and the entrained ambient air. Free shear layers are known to be unstable and can amplify perturbations that naturally present in or seeded into the flow over a range of frequencies. This instability is called Kelvin-Helmholtz instability. Detailed linear stability analyses [e.g. Michalke, 1965] have shown that the most amplified frequency scales with the momentum thickness of the boundary layer at the trailing edge of the splitter plate ($St_\theta = f_0\theta_0/U_j \sim 0.01$ to 0.02). Subsequent experimental investigations have shown that the initial waves due to K-H instability roll up into large-scale structures [Brown and Roshko, 1974]. These structures entrain fluid into the mixing layer from both sides and play a major role in the bulk mixing of fluids [Winant and Browand 1974]. Also, their dynamics are generally believed to be responsible for a significant portion of the far-field radiated noise [Moore 1977, Morse and McLaughlin 1979, Hileman et al. 2005].

An axisymmetric jet includes two additional instabilities. The first one is jet column instability. In an axisymmetric jet, the inward growth of the jet shear layer sets off azimuthal interactions around the jet axis. This interaction, which is dynamic and non-linear, is the source of jet column instability. The frequency of this instability is scaled with the nozzle exit diameter; $St_D = f_pD/U_j \sim 0.2$ to 0.6 [e.g. Crow and Champagne 1971, Hussain and Zaman, 1981]. The St_D of the jet preferred mode varies over a large range, but mostly hovers around 0.3 [Ho and Huerre, 1984]. The second one is azimuthal instability with various modes, which compete for energy and grow selectively [Cohen and Wygnanski 1987, Corke et al. 1991].

The main goal of the research at the Ohio State University has been the development and application of LAFPAs to the control of high-speed and high-Reynolds number jets. Initial development of the actuators can be found in Samimy et al. [2004], and later development in Utkin et al. [2007] and Samimy et al. [2007b]. The use of actuators for noise mitigation in Mach 0.9 jet and 1.3 perfectly-expanded jets can be found in Samimy et al. [2007a] and Kim et al. [2008], respectively. The actuators have also been used for mixing and jet structure manipulation in a perfectly-expanded Mach 1.3 jet [Samimy et al. 2007b]. While all the work discussed so far had been conducted in unheated jets, the work has recently been extended successfully to heated jets [Kearney-Fischer et al. 2008]. This paper will provide an overview of the research and is organized in the following fashion. Experimental facility and techniques will be discussed in Section 2; a brief description and characterization of actuators is presented in Section 3; sample results are presented and discussed in Section 4; and concluding remarks are offered in Section 5.

2. EXPERIMENTAL FACILITY AND TECHNIQUES

2.1 Jet Facility

All the experiments were conducted at the Gas Dynamics and Turbulence Laboratory at The Ohio State University. The ambient air is compressed, dried, and stored in two cylindrical tanks at a pressure of up to 16 MPa with a capacity of 36 m^3. The compressed air is supplied to the stagnation chamber and conditioned before entering into a nozzle. The air is discharged through the nozzle into an anechoic chamber and the directed outdoors (Fig. 1). A converging nozzle and two converging-diverging nozzles with design Mach numbers 1.3 and 2.0, designed using the method of characteristics, are used. The exit diameter of the nozzles is 2.54 cm (1.0”). A nozzle extension, made of boron nitride, is attached to the exit of the nozzle to house the plasma actuators. A Mach 1.65 nozzle with characteristics similar to those in a tactical aircraft is currently being designed and built. The jet facility is designed to accommodate laser-based flow diagnostics in a fully anechoic environment. Some results for perfectly-expanded Mach 1.3 jet will be presented and discussed in this paper.

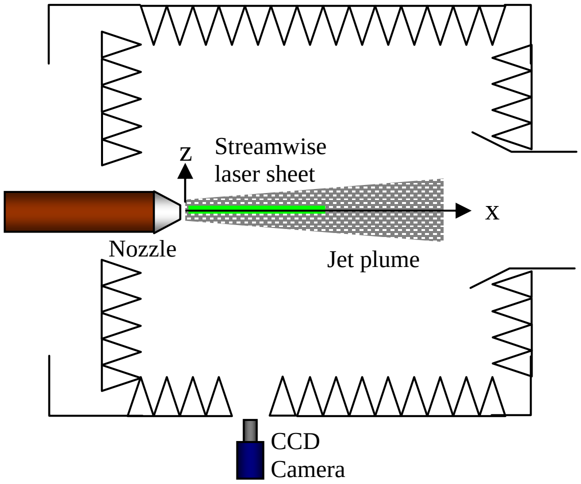

Figure 1: Schematic of the jet and the laser diagnostics set up. Not to scale.

The Reynolds number based on the nozzle exit diameter ranges from $0.7\text{x}10^6$ to $1.5\text{x}10^6$. The boundary layer at the exit of the nozzle is very thin, making it challenging to obtain a boundary layer profile to determine its momentum thickness and its state. With a Reynolds number of 0.7 million and higher, the boundary layers are expected to be turbulent. The critical Reynolds number to avoid the effects associated with low Reynolds number has been estimated to be about 0.4 million [Viswanathan 2004].

An electric heater-based storage heating system has been added to the jet facility recently. It consists of a 30 kW electric heater and a heat storage tank packed with rows of stainless steel plates spaced in such a way to allow air movement while efficiently imparting the desired temperature to the air. An electric fan takes the laboratory air, passes it through the electric heater, then through the heat storage tank, and discharges outdoors. When the steel plates in the heat storage tank are heated to the set temperature, the electronic control system shuts off the heating process. The electric heater has a maximum output temperature of about 870 K (1100 ºF), which produces a maximum jet stagnation temperature of about 800 K. During the heated jet experiments, the jet air passes through the heat storage tank, before entering the jet stagnation chamber. The jet experiments can be run continuously for approximately 20 to 40 minutes, depending upon the jet Mach number, with a temperature variation ~0.25 K/min.

1.2 Flow and Acoustic Diagnostics

Far-field sound pressure level (SPL) was measured using two ¼” B&K microphones, located at 30° and 90° relative to the jet axis. The far-field acoustic results were normalized to a radius of 80D. The acoustic signal from each microphone was conditioned, band-pass filtered from 20 Hz to 100 kHz, amplified by a four-channel B&K Nexus conditioning amplifier, and then sampled at 200 kHz per channel by a National Instruments A/D board. The window size was 8192 points providing a frequency resolution of 24.4 Hz. An average spectrum was obtained from one hundred spectra for each case.

A few flow diagnostic techniques have been utilized at GDTL. They include seeded perturbation development measurements using a Kulite pressure transducer grazing the shear layer of the jet in various streamwise locations; flow visualization using scattered laser light by submicron water particles formed in the mixing layer when the moisture in the entrained ambient air into the jet is cooled and condensed; and two-component particle imaging velocimetry (PIV) measurements. Details of the techniques can be found in Samimy et al. [2007a & b]. The jet was seeded with atomized oil particles in the unheated jet and aluminium oxide particles of 0.6 μm in the heated jet. For details of solid particle seeding technique, which is based on a technique developed by Wernet and Wernet [1994], see Kearney-Fischer et al. [2008].

3.0 LOCALIZED ARC FILAMENT PLASMA ACTUATORS

There has been a considerable interest in the use of electric discharge-based plasmas for flow control over the last decade. The work in this field has covered a wide range of experimental approaches and engineering applications. Various types of surface and volume-filling plasmas, including DC, AC, RF, microwave, arc, corona, spark electric discharges, and laser-induced breakdown, have been used in an effort to control flows. The primary mechanisms of plasma-based flow control include electrohydrodynamic (EHD) and magnetohydrodynamic (MHD) interactions, and thermal heating. EHD and MHD interactions involve flow entrainment by collisional momentum transfer from charged species accelerated by Coulomb and Lorentz forces, respectively. A brief discussion of the capabilities and limitation of these techniques as well of many references on the subject can be found in Utkin et al. [2007] and Samimy et al. [2007b]. LAFPA provides localized temperature perturbation of high amplitude and high bandwidth, which is a purely thermal effect. Various instabilities in the jet are manipulated using these perturbations to achieve mixing enhancement or noise mitigation. The present approach is not limited to low-speed flows (unlike EHD control) or low-pressure flows (unlike MHD control). In addition, it requires sufficiently low power for practical applications. In fact, the present approach is the only energy efficient, high-speed, standard (~sea level) static pressure flow control method, which has been demonstrated in experiments.

Each LAFPA consists of a pair of pin electrodes. The electrodes are distributed around the nozzle perimeter, as shown schematically in Fig. 2, approximately 1 mm upstream of the nozzle exit plane. A 0.5 mm deep and 1 mm wide ring groove was used to house the electrodes and to shield and stabilize the plasma. The plasma was swept downstream by the high momentum flow without such a groove. For the work presented here, the nozzle extension was made of boron nitride and tungsten wires of 1 mm diameter were used for electrodes. The spacing between a pair of electrodes in each actuator, center-to-center, is 3 mm.

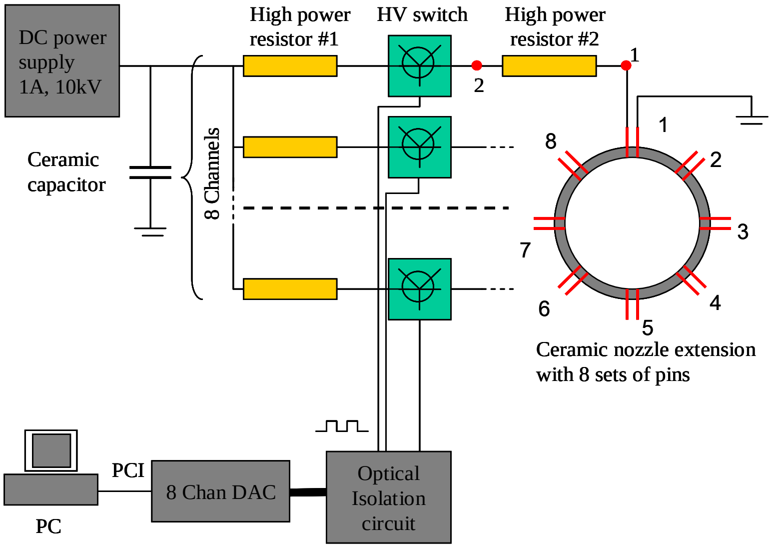

Figure 2: Schematic of the in-house fabricated plasma generator.

.

Figure 2 shows a schematic of the multi-channel high-voltage plasma generator, designed and built in-house at the Ohio State University. The current plasma generator enables simultaneous powering of up to eight localized actuators distributed around the perimeter of the ceramic nozzle extension, with independent frequency, duty cycle, and phase control of individual actuators. With eight actuators, azimuthal modes (m) 0, 1, 2, 3, ±1, ±2, and ±4 can be forced. When forcing the axisymmetric mode m=0, all the actuators are turned on at the same time. For the simple helical modes (m=1-3), there is a phase difference of $2\pi m/8$ between the adjacent actuators. The combined helical modes (m=±1, ±2, ±3) are obtained by superposition of the simple helical modes of opposite signs. The actuators can be operated over a wide bandwidth of 0 to 200 kHz, enabling the forcing of both the jet column and the jet initial shear layer instabilities.

By turning the electronic switch on and off, positive high voltage pulses can be applied to the corresponding actuator. The high initial voltage is needed to produce breakdown in the approximately atmospheric pressure air in the gap between the two electrodes of an actuator. After the breakdown, the arc is generated and the voltage across the gap rapidly falls to a few hundred volts. The average power used by an actuator in a typical operation is approximately 20 W (i.e. 160 W net power for all eight actuators in operation). For comparison, the flow power (the total enthalpy flux) at these conditions is about 28 kW – ratio of the average actuator to the flow power of 0.57%. This demonstrates that high-speed flow control by localized arc plasma actuators can be highly energy efficient. Detailed actuator characteristics can be found in Samimy et al. [2007a & b] and Utkin et al. [2007]. An RF based plasma generator system has been recently developed, which is light weight, energy efficient, and more amenable for application.

4. EXPERIMENTAL RESULTS

As was discussed, the jet behaves like an amplifier, selectively amplifying perturbations of certain modes over a range of frequencies. These selected perturbations grow into instability waves/flow structures, the extent of growth of which depends on the perturbation frequency; and the dynamics of largest scales are known to produce the peak far-field noise radiated to small angles with respect to the jet axis. It is also known that certain lower modes (e.g. m=0, 1) are much more efficient radiators of jet noise than higher azimuthal modes. However, there is a competition between these modes to extract energy from the jet in order to grow into large-scale structures and thus the growth of targeted modes can effectively suppress the growth of other modes. Therefore, the main function of using LAFPAs is to selectively enhance the structures that are less efficient noise radiators (and suppress the structures that are more efficient noise radiators) thereby reducing the far-field noise. Sample results of the seeded perturbation growth are shown in Section 4.1. The effects of forcing on the flow field and far-field noise are presented in Sections 4.2 and 4.3.

4.1 Seeded Perturbation Development

Development of seeded perturbations by LAFPAs is shown in Fig. 3 for various azimuthal modes at several forcing Strouhal numbers and compared with the development of natural perturbations in the baseline (unforced) jet. Several trends are observed:

- For the natural perturbations, there is a significant growth in lower Strouhal numbers followed by saturation around the end of the potential core (x/D~6). The natural perturbations of higher Strouhal numbers do not show any growth in the jet. This probably means that the jet column instability plays more significant role in the baseline jet than the initial shear layer instability.
- The perturbation amplitude at the first measurement point (x/D=0.5) keeps going up with the forcing Strouhal number, indicating significant growth of higher Strouhal number perturbations in the initial shear layer. Also, the location of the onset of the perturbation decay moves upstream as the forcing Strouhal number goes up. These results are consistent with the results in the literature, which show that the thin initial shear layer can support only the growth of higher Strouhal numbers perturbations;
- The overall trends for all four azimuthal modes are similar;
- In lower forcing Strouhal numbers, higher azimuthal modes saturate earlier and decay faster;
- All perturbations approach the baseline farther downstream;
- There is a strong competition between the axisymmetric and first helical modes – the latter seems to have upper hand in the lower frequencies and the role switches in the higher frequencies; and
- The growth and decay of the seeded perturbation are less dependent on the azimuthal modes at a higher Strouhal numbers. This is expected as the azimuthal modes are associated mostly with the jet column instability.

Moore (1977) performed similar experiments while using an acoustic driver to excite the jet preferred frequency in a low Mach number jet. He observed trends similar to the present trends. Some of these results and trends of the current work are also consistent with linear stability results of Michalke [1977 and Cohen and Wygnanski [1987] and experimental results of Cohen and Wygnanski [1987] and Corke et al. [1991]. The energy exchange between various azimuthal modes and the mean flow seems to be similar in the growth phase of instability wave/perturbation, but significantly different in the decay phase – the higher azimuthal modes decay much faster, especially in lower Strouhal number forcing. We were limited to m=3 with the current 8 actuators arrangement. We will use more actuators enabling us to excite higher azimuthal modes in the near future.

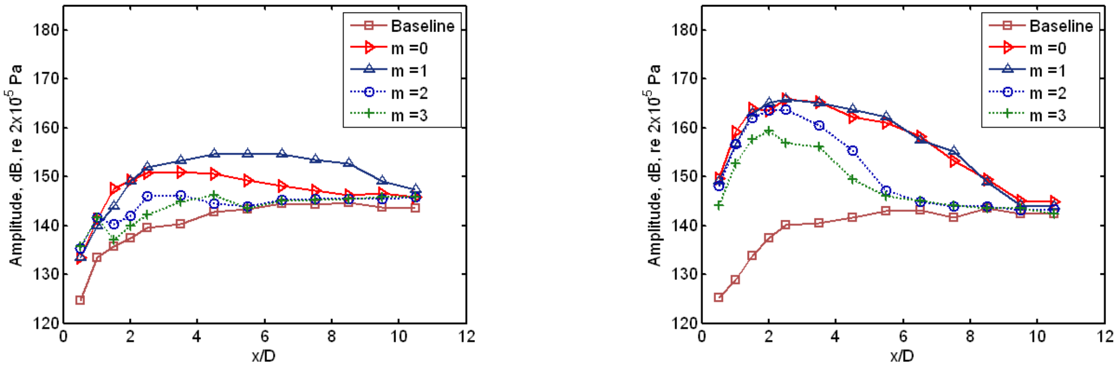

(a) St$_{DF}$ = 0.13 (b) St$_{DF}$ = 0.33

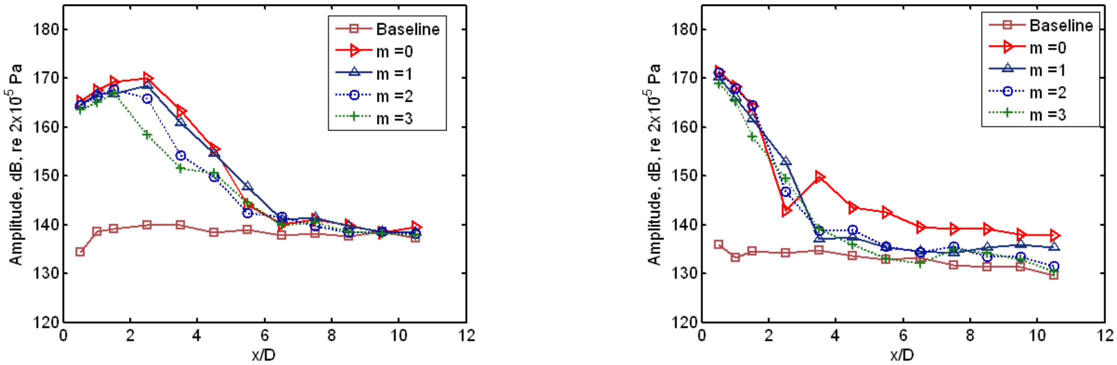

(c) St$_{DF}$ = 0.66 (d) St$_{DF}$ = 1.31

Figure 3: Effects of excitation mode on spatial development of seeded perturbation at several Strouhal numbers.

4.2 Flow Field Results

Detailed flow visualization and velocity measurements have been carried out to understand the effects of forcing on large-scale structures in the jet [Samimy et al. 2007b, Kim and Samimy 2008, Kearney-Fischer et al. 2008]. Figure 4 shows typical PIV results - Galilean streamlines (coordinate system travelling with the convective velocity) superimposed on velocity magnitude for the baseline jet and at three forcing Strouhal numbers at azimuthal mode m = ±1. This technique is used to visualize flow structures [Kline and Robinson 1990]. As can be seen in Fig. 4 (a), the baseline jet contains large-scale structures, but they lack organization. Forcing the jet around the jet column instability Strouhal number (~0.3) generates very strong and coherent structures similar to those that have been observed in low-speed and low Reynolds number flows (Fig. 4 (c)). Forcing the jet with lower or higher Strouhal numbers generates larger and smaller structures, respectively, but not as organized. As it is obvious from these results, dynamics of flow structures, and thus far-field radiated noise, can be controlled by using LAFPAs. The main goal of the research at GDTL is to understand the processes involved and thus to judiciously use this control technique for maximum noise mitigation.

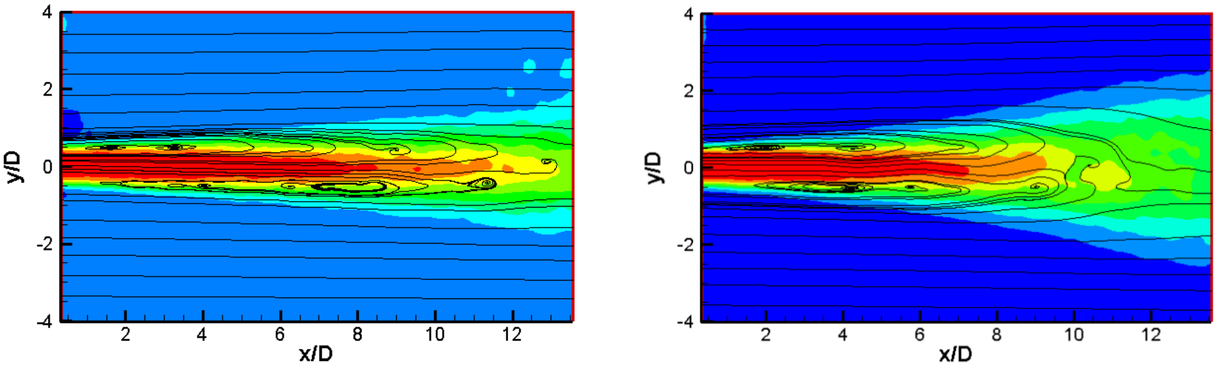

(a) Baseline

(b) $St_{DF} = 0.20$

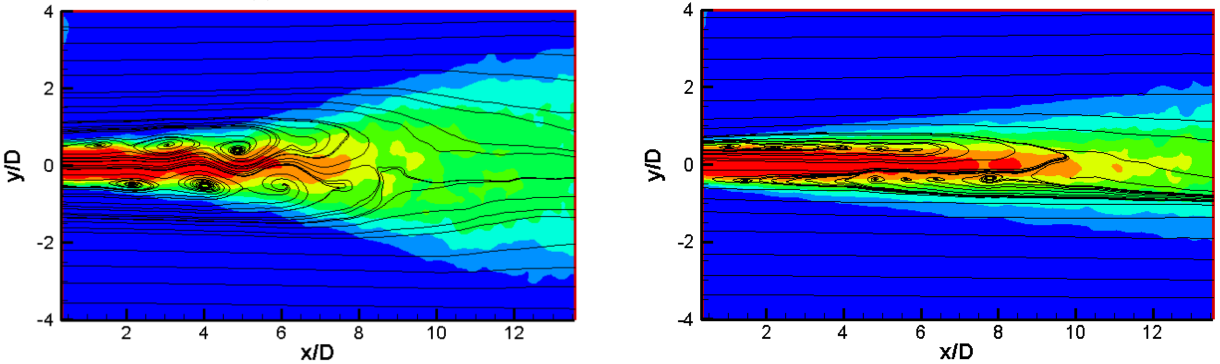

(c) $St_{DF} = 0.33$

(d) $St_{DF} = 1.05$

Figure 4: Galilean streamlines superimposed on the streamwise velocity magnitude for the baseline Mach 1.3 jet and for forcing azimuthal mode m = ±1.

4.3 Far-Field Acoustic Results

Detailed far-field acoustic measurements have been carried out in an unheated perfectly-expanded Mach 1.3 jet, along with limited measurements in several heated cases. The forcing azimuthal modes include m = 0-3, ±1, ±2, and ±4 over Strouhal number of 0.07 to 5. Spectra (normalized to 80D) for the baseline jet are shown in Fig. 5 at polar angles of 30° and 90° with respect to the jet axis. Although the jet was perfectly expanded, there are indications of shock associated noise in both cases – there are two tones of small amplitude at 30° and both tones and broadband shock noise at 90°. There are always weak waves in a supersonic jet, no matter how carefully the nozzle exit pressure and the ambient pressure are matched, which interact with the large-scale structures in the jet to generate broadband noise, as seen at the 90° case. In addition, the nozzle extension, which holds the actuators, has a very thick lip. This can reflect the upstream radiated shock generated noise and set up a natural feedback-loop causing the development of the tones, as seen at both 30° and 90°.

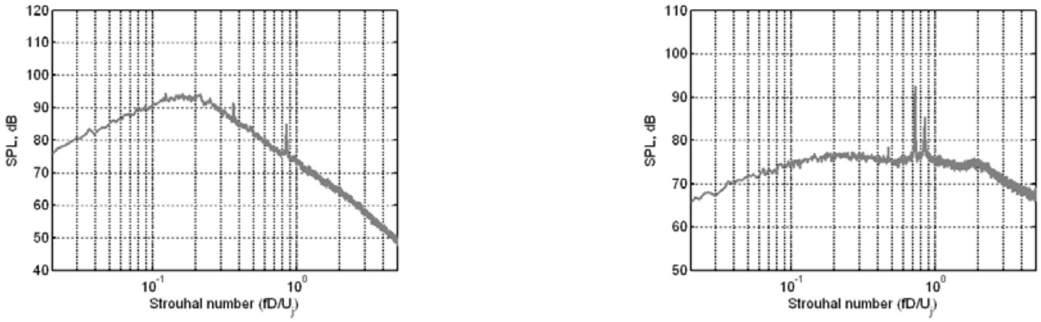

(a) Baseline spectrum at 30°

(b) Baseline spectrum at 90°

Figure 5: Far-field acoustic spectra at 30° and 90° with respect to the jet axis for the baseline Mach 1.3 jet.

Figure 6 shows the effects of forcing on the far-field acoustics at several forcing Strouhal numbers for the axisymmetric azimuthal mode, m = 0, at 30°. The forcing Strouhal number location on each graph is identified by two triangles. At this mode, the forcing tone and its harmonics are strong, and there is a significant noise increase in lower forcing Strouhal numbers, in agreement with the results in the literature. The peak mixing noise level started to decrease beyond St_{DF} of about 0.7 and the maximum reduction was observed at St_{DF} = 1.6 (not shown here). As the St_{DF} is increased beyond this value, the reduction in the peak mixing noise level is decreased. The maximum noise increase over a large Strouhal number (St_D>0.4) occurs when the jet is forced at St_{DF} = 0.27, which is near that of the jet column instability. These results are consistent with the flow field results (shown in Fig. 4) and with the perturbation growth results (shown in Fig. 3).

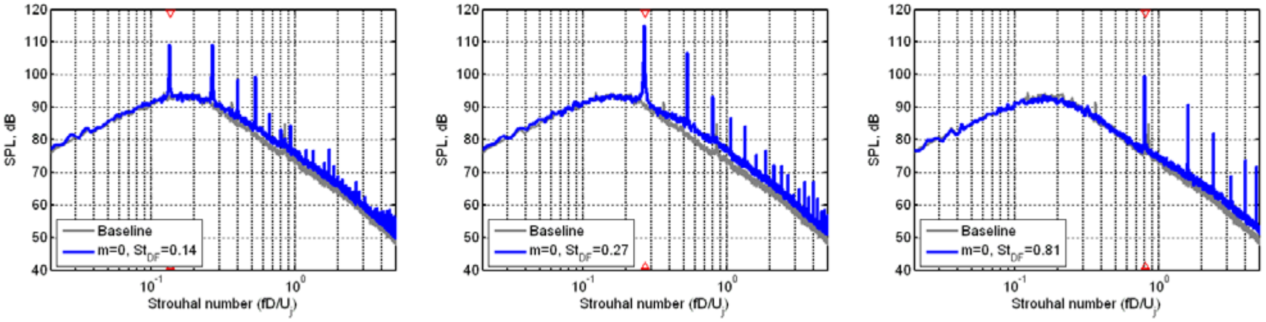

(a) St_{DF} = 0.14

(b) St_{DF} = 0.27

(c) St_{DF} = 0.81

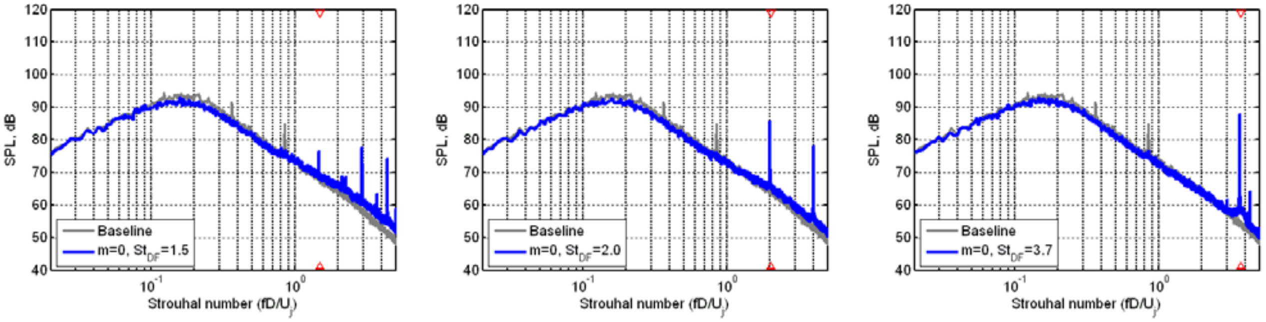

(d) St_{DF} = 1.5

(e) St_{DF} = 2.0

(f) St_{DF} = 3.7

Figure 6: Far-field spectra at 30° at several forcing Strouhal numbers for m = 0.

At 90° location (not shown here), the forcing at m = 0 does not seem to have any noticeable effect on the broadband noise in lower forcing Strouhal numbers, even at forcing Strouhal number close to that of jet column instability, there is a significant noise reduction over almost the entire spectrum at higher forcing Strouhal number [Kim et al. 2008].

Figure 7 shows the effects of forcing on the acoustic spectrum at 30° at several forcing Strouhal numbers for the azimuthal mode m = 3, which is the highest simple azimuthal mode attainable with the 8 actuators arrangement currently used at GDTL. At low forcing Strouhal numbers, there is no tone at the forcing Strouhal number, but there are relatively weak tones at its harmonics. At forcing Strouhal numbers lower than about 0.14, the effect of forcing is negligible (not shown). The peak mixing noise, centered at Strouhal number of about 0.2, starts to decrease at St_{DF} of about 0.27. The maximum reduction in the peak mixing noise is about 4 dB at St_{DF} of about 0.8. As the St_{DF} is increased further, the amount of reduction in the peak mixing noise is deceased slowly similar to the m = 0 forcing case. The effect of forcing on the far-field spectra at 90˚ are shown in Fig. 8 for m = 3 for three forcing Strouhal numbers. At forcing Strouhal number less than about 0.3, the broadband noise level was slightly increased over a large Strouhal number range (Fig. 8 (a)). For forcing Strouhal number from 0.3 to 2.4, the broadband noise level was reduced at Strouhal numbers less than that of the tone in the baseline jet, but either increased or remained the same above that (Fig. 8 (b)). The broadband noise level was reduced in the entire span of the Strouhal number at higher than 2.4 forcing Strouhal number.

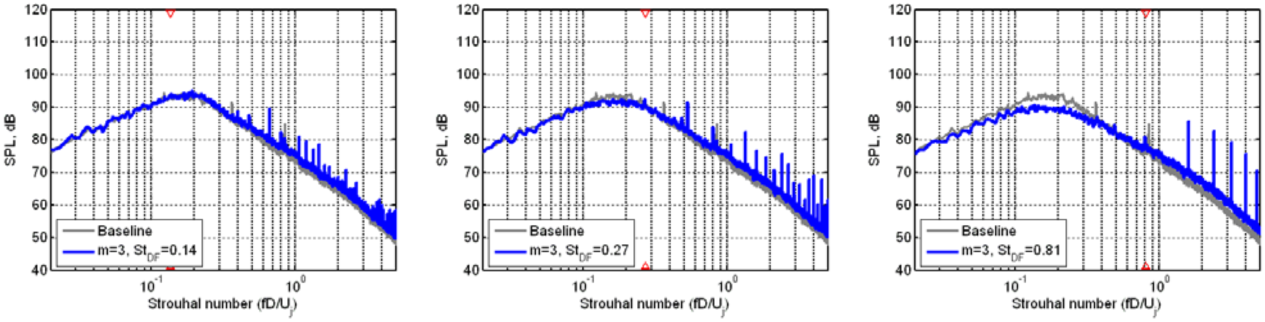

(a) St_{DF} = 0.14 (b) St_{DF} = 0.27 (c) St_{DF} = 0.81

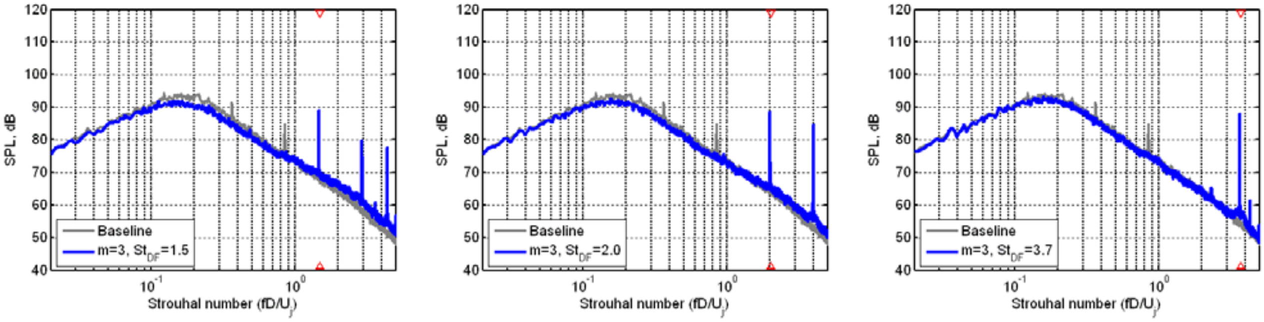

(d) St_{DF} = 1.5 (e) St_{DF} = 2.0 (f) St_{DF} = 3.7

Figure 7: Far-field spectra at 30° at several forcing Strouhal numbers for m = 3.

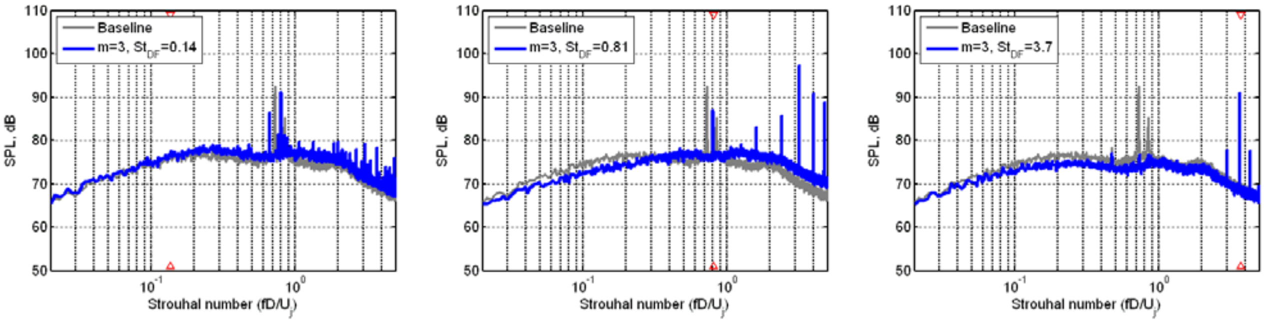

(a) $St_{DF} = 0.14$ (b) $St_{DF} = 0.81$ (c) $St_{DF} = 3.7$

Figure 8: Far-field spectra at 90° at several St_{DF}'s for m = 3.

Limited experiments carried out at NASA's Nozzle Acoustic Test Rig (NATR) with a nozzle exit diameter of 19.8 cm (7.8'') to explore the scalability of the technique. In LAFPAs, the distance between two electrodes of an actuator is limited to about 3 mm (2-5 mm). Therefore, number of actuators is expected to increase proportional to the nozzle exit diameter. However, in NASA experiments, we had an 8-channel power supply and could use only 8 actuators. This obviously put tremendous restriction on what could be done. More experiments are being planned at NASA as well as GE for more detailed experiments. It was observed at NATR experiments that the amplitude of excitation tone remained about the same as in the much smaller GDTL facility [Samimy et al. 2006]. Therefore, their importance is expected diminish in practical engines. For this reason and also just to assess the effects of forcing on broadband noise, the forcing tones are removed in calculating the Overall Sound Pressure Level (OASPL). This has also been done in the literature [Moore 1977].

The OASPL was calculated for Strouhal numbers from 0.01 to 4 to evaluate the effects of forcing on the broadband noise reduction. The results are shown in Fig. 9 at 30° and 90°. The overall trend of the OASPL variation with St_{DF} is very similar to what was observed in a Mach 0.9 jet [Samimy et al. 2007a]. At low forcing Strouhal numbers, the OASPL was increased by plasma actuators at both angles. As was shown earlier in Fig. 4, well organized robust, large-scale structures were generated in an orderly fashion at low forcing Strouhal numbers. This enhanced dynamics of large-scale are responsible for the increased noise.

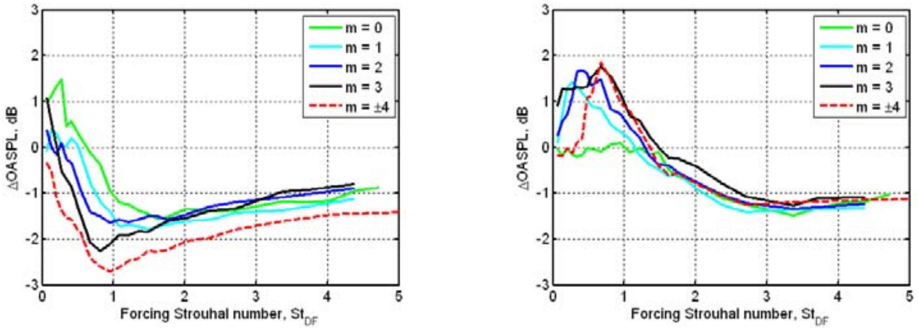

(a) 30˚ (b) 90˚

Figure 9: Change in OASPL due to excitation relative to the baseline jet.

At 30˚ location, the dominant noise component is mixing noise believed to be generated by the dynamics of large-scale structures near the end of potential core. As a result, making the structures more organized and thus their interaction more dynamic is expected to increase the peak noise. On the other hand, making them more benign is expected to decrease the peak noise. Thus the reduction in peak mixing noise shown in Figs. 6

and 7 is directly related to the OASPL reduction. The maximum reduction in OASPL is increased as the mode number is increased from m =0 or 1 to 3, similar to the results in Mach 0.9 jet [Samimy et al. 2007a]. The maximum reduction is about 2.2 dB at m = 3 mode. This is a slightly greater reduction than obtained in Mach 0.9 jet. For mixed modes, more reduction was observed compared to the simple modes. The maximum reduction at m = ±2 (not shown here) is comparable to m = 3 and a greater reduction of 2.7 dB is observed at m = ±4.

At the sideline location of 90˚, the maximum reduction was observed at much higher forcing Strouhal number than those at 30˚. It seems that the maximum reduction occurs at around St$_{DF}$ of 3.4 for all modes. At this high St$_{DF}$, the effects of mode appear to be negligible. For mixed modes, about the same level of reduction was found for all modes, but the reduction seemed slightly greater for m = ±2 and ±4. At this location, the maximum reduction for each mode is about the same and thus does not depend much on the mode, as expected. The trend of the variation in OASPL with St$_{DF}$ is similar to what was found in the Mach 0.9 jet [Samimy et al. 2007a].

Limited far-field acoustics results have also been obtained for heated Mach 1.3 jet over a large range of forcing Strouhal number, but in two stagnation temperature ratios and only for azimuthal mode m = 3, which has been shown to be the best azimuthal mode (using the available 8 actuators) for noise suppression based on the unheated jet results (Fig. 9). The results presented in Fig. 10 show the difference in the overall sound pressure level between the forced jet and the baseline (unforced) jet at 30° and 90°. Note that the temperature ratio of 1 is for the unheated jet shown in Fig. 9. These preliminary results are very encouraging, as the performance of the actuators in the heated jet is much better than in the unheated jet in both observation angles (by about 0.5 dB at 30° and about 1 dB at 90°).

While the results are preliminary and more work is underway, there are two likely rationales for the improved effectiveness of the LAFPAs at the elevated temperatures. The first one is related to the interaction of the initial shear layer instability (ISLI) and the jet column instability (JCI). As discussed earlier, at the forcing Strouhal number of around 0.3, LAFPAs excite the jet column instability. However, it has been shown in the literature in low-speed and low Reynolds number flows that when the ISLI frequency approaches an even multiple of the JCI frequency (i.e. $f_{ISLI} \sim 2^n f_{JCI}$, where n is normally 3), multiple pairings of the initial instability waves/structures take place that drops the initial frequency/increases the initial wave length to match that of the JCI frequency/wave length (Samimy et al. 2007b, Ho & Huerre 1984, and Kibens 1980). This causes a sort of resonance that increases the mixing and entrainment. The second potential reason is that heating the jet changes the initial momentum thickness and thus f_{ISLI}, moving the system closer to this resonance situation. These issues are currently under further exploration.

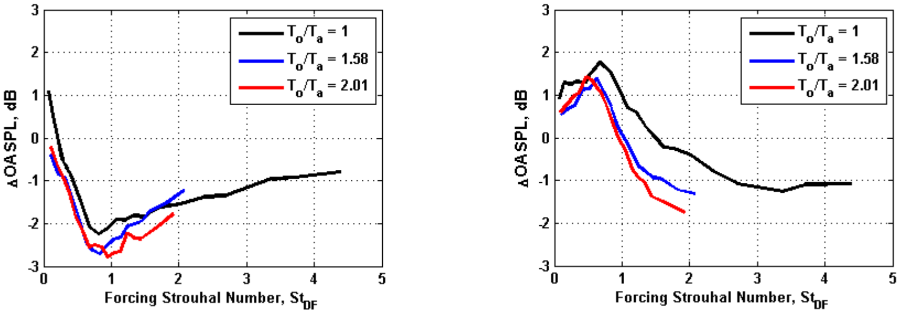

(a) 30˚ (b) 90˚

Figure 10: Change in the OASPL, relative to the baseline jet, due to excitation at m = 3 for three temperature ratios.

5. Concluding Remarks

A brief overview of the localized arc filament plasma actuators, which have recently been developed at the Ohio State University, was provided. These actuators have very large bandwidth of 0 to 200 kHz and provide high amplitude perturbations that are used for manipulation of instabilities of the jet for noise mitigation as well as mixing enhancement. These actuators provide localized heating and are very different than those based on electromagnetic or electrohydrodynamic principles. A brief review of some of the recent work at GDTL using these actuators in both subsonic and supersonic high Reynolds number jets was also provided. Sample results in a Mach 1.3 ideally expanded unheated as well as heated jet were presented and discussed. The results included seeded perturbation development, velocity field, and far-field noise, which collectively show that forcing the jet with low frequency and low azimuthal modes generates more noise and with higher frequency and higher azimuthal modes provides noise mitigation. In the former, perturbations grow quickly, but decay very slowly contributing to the far-field noise. In the latter, the growth of perturbation is still rapid, but they decay very rapidly generating much less noise.

Acknowledgements

The research is supported by NASA and also recently by a Navy SBIR. The support of and fruitful discussions with James Bridges and Cliff Brown of NASA Glenn Research Center; Steve Martens of GE; Sivaram Gogineni of Spectral Energies; and Aniruddha Sinha and Munetake Nishihara of OSU are greatly appreciated.

References

[1] Ahuja, K.K., Lepicovsky, J. and Burrin, R.H., “Noise and Flow Structure of a Tone-Excited Jet,” *AIAA Journal*, Vol. 20, No. 12, 1982, pp 1700-1706.

[2] Brown, G.L. and Roshko, A., “On Density Effects and Large Structure in Turbulent Mixing Layers,” *Journal of Fluid Mechanics*, Vol. 64, 1974, pp.715-816.

[3] Cohen, J., and Wygnanski, I., “The evolution of instabilities in the axisymmetric jet. Part 1. The linear growth of disturbances near the nozzle,” *Journal of Fluid Mechanics*, Vol. 176, 1987, pp191-219.

[4] Corke, T.C., Shakib, F. and Nagib, H.M., “Mode selection and resonant phase locking in unstable axisymmetric jets,” *Journal of Fluid Mechanics*, Vol. 223, 1991, pp. 253-311.

[5] Crow, S. and Champagne, F., “Orderly Structure in Jet Turbulence,” *Journal of Fluid Mechanics*, Vol. 48, 1971, pp. 547-591.

[6] Hileman, J., Thurow, B.S., Caraballo, E.J. and Samimy, M., “Large-Scale Structure Evolution and Sound Emission in High-Speed Jets: Real-Time Visualization with Simultaneous Acoustic Measurements,” Journal of Fluid Mechanics, Vol. 544, 2005, pp. 277-307.

[7] Ho, C.-M. and Huerre, P., “Perturbed Free Shear Layers,” *Annual Review of Fluid Mechanics*, Vol. 16, 1984, pp. 365-424.

[8] Hussain, A.K.M.F. and Zaman, K.B.M.Q., “The ‘preferred mode’ of the axisymmetric jet,” *Journal of Fluid Mechanics*, Vol. 110, 1981, pp. 39-71.

[9] Jubelin, B., "New Experimental Studies on Jet Noise Amplification," *AIAA Paper 80-0961*, 1980.

[10] Kearney-Fischer, M., Kim, J.-H. and Samimy, M., "Control of a Heated High Reynolds Number Mach 0.9 Jet Using Plasma Actuators," AIAA Paper No. 2008-3874, June 2008.

[11] Kibens, V., "Discrete Noise Spectrum Generated by an Acoustically Excited Jet," AIAA J*ournal*, Vol. 18, 1980, pp 434-451.

[12] Kim, J.-H., Adamovich, I., and Samimy, M. "Active Noise Control in a Mach 1.3 Ideally-Expanded Jet with Plasma Actuators," AIAA Paper No. 2008-0038, January 2008.

[13] Kim, J.-H. and Samimy, M., "Effects of Active Control on the Flow Structure in a High Reynolds Number Supersonic Jet," AIAA Paper No. 2008-3876, June 2008.

[14] Kline, S. J.; Robinson, S. K., "Quasi-coherent structures in the turbulent boundary layer. I - Status report on a community-wide summary of the data," Near-wall turbulence: 1988 Zoran Zaric Memorial Conference, Edited by S.J. Kline, N.H. Afgan, 1990**.**

[15] Lighthill, M. J., "On sound generated aerodynamically II. Turbulence as a sound source," *Proceeding of Royal Society of Lon*don, Vol. 222, pp. 1-32, 1954.

[16] Martens, S. and Haber, Ludwig, "Jet Noise Reduction for High Speed Exhaust Systems," GT2008-50455, Berlin, Germany, June 2008.

[17] Michalke, A., "On Spatially Growing Disturbances in an Inviscid Shear Layer," *Journal of Fluid Mechanics*, Vol. 23, 1965, pp. 521-544.

[18] Moore, C.J., "The role of shear-layer instability waves in jet exhaust noise," *Journal of Fluid Mechanics*, Vol. 80, 1977, pp. 321-367.

[19] Morrison, G. & McLaughlin, D., "Noise Generation by Instabilities in Low Reynolds Number Supersonic Jets," *Journal of Sound and Vibration*, Vol. 65, 1979, pp. 177-191.

[20] Samimy, M., Adamovich, I., Webb, B., Kastner, J., Hileman, J., Keshav, S. and Palm, P., "Development and Characterization of Plasma Actuators for High Speed Jet Control", *Experiments in Fluids*, Vol. 37, No. 4, 2004, pp. 577-588.

[21] Samimy, M., J., Kim, Kastner, J.-H., Adamovich, I., and Utkin, Y., "Active Control of a Mach 0.9 Jet for Noise Mitigation Using Plasma Actuators," AIAA Journal, Vol. 45, No. 4, pp. 890-901, 2007a.

[22] Samimy, M., Kim, J.-H., Kastner, J., Adamovich, I., and Utkin, Y., "Active Control of High Speed and High Reynolds Number Jets Using Plasma Actuators," Journal of Fluid Mechanics, Vol. 578, pp. 305-330, May 2007b.

[23] Samimy, M., Debiasi, M., Caraballo, E., Serrani, A., Yuan, X., Little, J., and Myatt, J., "Feedback Control of Subsonic Cavity Flows Using Reduced-order Models," Journal of Fluid Mechanics, Vol. 579, pp. 315-346, May 2007c.

[24] Utkin, Y., Keshav, S., Kim, J.-H., Kastner, J., Adamovich, I., and Samimy, M., "Use of Localized Arc Filament Plasma Actuators for High Speed Jet Control," Journal of Physics D: Applied Physics, Vol. 40, pp. 685-694, February 2007.

[25] Viswanathan, K., "Aeroacoustics of Hot Jets", Journal of Fluid Mechanics, Vol. 516, pp. 39-82, 2004.

[26] Wernet, J. & Wernet, M., 1994, "Stabilized alumina/ethanol colloidal dispersion for seeding high temperature are flows," *Proc. of ASME Symp. on Laser Anemometry: Advances and Applications.*

[27] Winant, C.D. and Browand, F.K., "Vortex Pairing: The mechanism of Turbulent Mixing-Layer Growth at Moderate Reynolds Number," *Journal of Fluid Mechanics*, Vol. 63, 1974, pp. 237-252.

[28] Zaman, K.B.M.Q. and Hussain, A.K.M.F., "Vortex pairing in a circular jet under controlled excitation. Part 1. General Jet Response," *Journal of Fluid Mechanics*, Vol. 101, part 3, 1980, pp.449-491.